Neuroestrogens facilitate male-typical behaviors by potentiating androgen receptor signaling in medaka

Yuji Nishiike[1], Shizuku Maki[1], Daichi Miyazoe[1], Kiyoshi Nakasone[1], Yasuhiro Kamei[2], Takeshi Todo[3], Tomoko Ishikawa-Fujiwara[3], Kaoru Ohno[4], Takeshi Usami[4], Yoshitaka Nagahama[4], and Kataaki Okubo[1,*]

[1]Department of Aquatic Bioscience, Graduate School of Agricultural and Life Sciences, The University of Tokyo, Bunkyo, Tokyo 113-8657, Japan

[2]Optics and Bioimaging Facility, Trans-Scale Biology Center, National Institute for Basic Biology, Okazaki, Aichi 444-8585, Japan

[3]Department of Genome Biology, Graduate School of Medicine, Osaka University, Suita, Osaka 565-0871, Japan

[4]Division of Reproductive Biology, National Institute for Basic Biology, Okazaki, Aichi 444-8585, Japan

***Corresponding author:** Kataaki Okubo; Tel: +81-3-5841-5288. Fax: +81-3-5841-5289. E-mail: a-okubo@g.ecc.u-tokyo.ac.jp.

Abstract

In rodents, estrogens aromatized from androgens in the brain, also known as neuroestrogens, are essential for the development of male-typical behaviors. In many other vertebrates including humans and teleost fish, however, androgens facilitate these behaviors directly via the androgen receptor without aromatization into estrogens. Here we report that male medaka fish lacking Cyp19a1b (a subtype of aromatase predominantly expressed in the brain) exhibit severely impaired male-typical mating and aggression, despite elevated brain androgen levels. These phenotypes can be rescued by estrogen administration, indicating that neuroestrogens are pivotal for male-typical behaviors even in non-rodents. Our results further suggest that neuroestrogens facilitate male-typical behaviors by potentiating androgen action in the brain via the direct stimulation of androgen receptor transcription, thereby revealing a previously unappreciated mechanism of action of neuroestrogens. We additionally show that female fish lacking Cyp19a1b are less receptive to male courtship and conversely court other females, highlighting the significance of neuroestrogens in establishing sex-typical behaviors in both sexes.

Keywords: aggression; androgen receptor; aromatase; mating; neuroestrogen

Introduction

Male and female animals exhibit differences in many innate behaviors, such as mating and aggression (1). In vertebrates, these differences are driven primarily by the influence of sex steroid hormones, including estrogens and androgens. Extensive research in rodents has established that estrogens, traditionally considered "female" hormones, are critical for the development of male-typical behaviors (2–4). Specifically, androgens secreted by the testis, both perinatally and in adulthood, are converted to estrogens in the brain by the enzyme aromatase. These brain-derived estrogens, also called neuroestrogens, then act through ESR1, a subtype of the estrogen receptor (ESR), to elicit male-typical behaviors (2–4). This process, originally referred to as the "aromatization hypothesis", is now widely accepted as correct; however, the mechanisms through which neuroestrogens affect male-typical behavior, including the identity of their downstream targets, remain largely elusive (4, 5).

More importantly, the aromatization hypothesis seems to apply to only a limited number of species besides rodents (e.g., some birds such as zebra finches) (6). In other species such as humans, other primates, and teleost fish, testicular androgens facilitate male-typical behaviors directly through the androgen receptor (AR) without aromatization (7–9). Notably, in teleosts, 11-ketotestosterone (11KT), which cannot be aromatized to estrogens, is the primary testicular androgen, and exogenous 11KT effectively induces male-typical courtship and aggression even in females (9–11). Therefore, it is generally assumed that, in teleosts, androgens are solely responsible for male-typical behaviors, while estrogens are dispensable for these behaviors. This is consistent with the recent finding in medaka fish (*Oryzias latipes*) that estrogens act through the ESR subtype Esr2b to prevent females from engaging in male-typical courtship (10).

Interestingly, despite these findings, adult teleost brains have extremely high levels of aromatase activity (100–1000 times higher than in rodent brains), resulting in large amounts of neuroestrogens even in males (12). This observation suggests that neuroestrogens have a vital, but as yet undetermined, role in male teleosts. Most teleost species have two distinct genes encoding aromatase, *cyp19a1a* and *cyp19a1b*, due to a whole-genome duplication that occurred early in teleost evolution (12, 13). These genes have undergone subfunctionalization through the partitioning of tissue-specific expression patterns: *cyp19a1a* is expressed predominantly in the gonad, whereas *cyp19a1b* is expressed in the brain (12, 13).

In the present study, we generated *cyp19a1b*-deficient medaka, in which neuroestrogen synthesis is selectively impaired while gonadal estrogen synthesis remains intact, in order to investigate the impact of neuroestrogens on male behaviors. Contrary to our expectations, the fish showed severely impaired male-typical behaviors, thus revealing the marked behavioral effects of neuroestrogens. Our results further suggest that these effects are mediated by potentiating androgen signaling in behaviorally relevant brain regions.

71 # Results

72

73 ### *cyp19a1b*-deficient males exhibit severely impaired male-typical mating and
74 aggressive behaviors

75 We generated a *cyp19a1b*-deficient medaka line from a mutant founder carrying a nonsense
76 mutation in exon 4 of *cyp19a1b* that was identified through screening of the medaka TILLING
77 (targeting-induced local lesions in genomes) library (14) (Fig. S1, A and B). Loss of *cyp19a1b* function
78 in these fish was verified by measuring brain and peripheral levels of sex steroids. As expected, brain
79 estradiol-17β (E2) in both male and female homozygous mutants (*cyp19a1b*$^{-/-}$) was significantly
80 reduced to 16% and 50%, respectively, of the levels in their wild-type (*cyp19a1b*$^{+/+}$) siblings ($P = 0.0037$,
81 males; $P = 0.0092$, females) (Fig. 1, A and B). In males, brain E2 in heterozygotes (*cyp19a1b*$^{+/-}$) was
82 also reduced to 45% of the level in wild-type siblings ($P = 0.0284$) (Fig. 1A). In contrast, peripheral E2
83 levels were unaltered in both *cyp19a1b*$^{-/-}$ males and females (Fig. S1, C and D), consistent with the
84 expected functioning of Cyp19a1b primarily in the brain. Brain levels of testosterone, as opposed to E2,
85 increased 2.2-fold in *cyp19a1b*$^{-/-}$ males relative to wild-type siblings ($P = 0.0006$) (Fig. 1A). Similarly,
86 brain 11KT levels in *cyp19a1b*$^{-/-}$ males and females increased 6.2- and 1.9-fold, respectively, versus
87 wild-type siblings ($P = 0.0007$, males; $P = 0.0316$, females) (Fig. 1, A and B). Their peripheral 11KT
88 levels also increased 3.7- and 1.8-fold, respectively ($P = 0.0789$, males; $P = 0.0118$, females) (Fig. S1,
89 C and D). These results show that *cyp19a1b*-deficient fish have reduced estrogen levels coupled with
90 increased androgen levels in the brain, confirming the loss of *cyp19a1b* function. They also suggest that
91 the majority of estrogens in the male brain and half of those in the female brain are synthesized locally
92 in the brain.

93 Next, we investigated the mating behavior of *cyp19a1b*-deficient males (Fig. 1C). The mating
94 behavior of medaka follows a stereotypical pattern, wherein a series of followings, courtship displays,
95 and wrappings by the male leads to spawning (15). Because 11KT, the primary driver of male-typical
96 behaviors in teleosts, was increased in *cyp19a1b*-deficient males, we predicted that these fish would
97 engage more actively in mating. Contrary to this expectation, however, *cyp19a1b*$^{-/-}$ males showed
98 significantly longer latencies to initiate wrappings ($P = 0.0033$ versus *cyp19a1b*$^{+/+}$, $P = 0.0195$ versus
99 *cyp19a1b*$^{+/-}$) and to spawn ($P = 0.0051$ versus *cyp19a1b*$^{+/+}$, $P = 0.0195$ versus *cyp19a1b*$^{+/-}$) (Fig. 1D),
100 suggesting that they are less motivated to mate.

101 However, no significant differences were evident in latencies to initiate followings and courtship
102 displays (Fig. 1D); therefore, the possibility that *cyp19a1b*-deficient males are less sexually attractive
103 and less preferred by females could not be ruled out. To ascertain whether *cyp19a1b*-deficient males are
104 indeed less motivated to mate, we further tested their mating behavior using *esr2b*-deficient females,
105 which are unreceptive to male courtship (10), as stimulus females (Fig. 1E); this test eliminates the
106 influence of female receptivity, facilitating an exclusive evaluation of male motivation to mate with
107 females (15). We found that *cyp19a1b*$^{-/-}$ males showed significantly longer latencies to initiate
108 followings ($P = 0.0129$ versus *cyp19a1b*$^{+/+}$, $P = 0.0060$ versus *cyp19a1b*$^{+/-}$), courtship displays ($P =$

109 0.0003 versus *cyp19a1b*$^{+/+}$, P = 0.0006 versus *cyp19a1b*$^{+/-}$), and wrapping attempts (P = 0.0009 versus
110 *cyp19a1b*$^{+/+}$, P = 0.0282 versus *cyp19a1b*$^{+/-}$) (Fig. 1F). In addition, they exhibited significantly fewer
111 courtship displays (P < 0.0001 versus both *cyp19a1b*$^{+/+}$ and *cyp19a1b*$^{+/-}$) and wrapping attempts (P <
112 0.0001 versus both *cyp19a1b*$^{+/+}$ and *cyp19a1b*$^{+/-}$) (Fig. 1G). These results thus confirmed that *cyp19a1b*-
113 deficient males are less motivated to mate. In our previous study, we found that *esr2b*-deficient females
114 court females preferentially over males (10). Consistent with that finding, here we observed that 12 of
115 15 *cyp19a1b*$^{+/+}$ females received courtship displays from the *esr2b*-deficient female, as compared with
116 only 2 of 15 *cyp19a1b*$^{+/+}$ males (P = 0.0003) (Fig. 1H). Curiously, we further observed that 8 of 15
117 *cyp19a1b*$^{-/-}$ males received courtship displays from the *esr2b*-deficient female (P = 0.0321 versus
118 *cyp19a1b*$^{+/+}$ males) (Fig. 1H). Perhaps *cyp19a1b*$^{-/-}$ males are misidentified as females by *esr2b*-deficient
119 females because they are reluctant to court or they exhibit some female-like behavior.
120 Next, we examined the intrasexual aggressive behavior of *cyp19a1b*-deficient males (Fig. 1I). The
121 aggressive behavior of teleosts including medaka consists of five types of behavioral acts: chases, fin
122 displays, circles, strikes, and bites (16). Again, contrary to our expectation, *cyp19a1b*$^{-/-}$ males exhibited
123 all of these aggressive acts less frequently than *cyp19a1b*$^{+/+}$ and/or *cyp19a1b*$^{+/-}$ males, with significant
124 differences observed for chases (P = 0.0123 versus *cyp19a1b*$^{+/-}$), fin displays (P = 0.0214 versus
125 *cyp19a1b*$^{+/+}$), and bites (P = 0.0015 versus *cyp19a1b*$^{+/+}$, P = 0.0002 versus *cyp19a1b*$^{+/-}$) (Fig. 1J). These
126 observations demonstrate that *cyp19a1b*-deficient males are less aggressive toward other males.
127 In tilapia (*Oreochromis niloticus*), depletion of *cyp19a1b* has been reported to cause male infertility
128 due to efferent duct obstruction (17). If this is also the case in medaka, the observed behavioral defects
129 might be secondary to infertility. We therefore investigated the fertilization and hatching success of
130 embryos derived from mating between *cyp19a1b*$^{-/-}$ males and wild-type females. Their fertilization and
131 hatching rates were 88.5% (n = 183) and 93.2% (n = 162), respectively, indicating that *cyp19a1b*-
132 deficient male medaka have normal fertility.
133

134 **Neuroestrogens facilitate male-typical behaviors probably by stimulating brain AR**
135 **expression**

136 We considered that the impaired male-typical behaviors of *cyp19a1b*-deficient males might be
137 reasonably attributed to either reduced E2 or increased 11KT in the brain. The latter possibility seemed
138 unlikely because 11KT/AR signaling strongly promotes male-typical behaviors in teleosts (15, 18);
139 therefore, we tested the former possibility by examining whether E2 treatment would rescue the
140 behavioral phenotypes of *cyp19a1b*-deficient males (Fig. 2A). E2 treatment, while having no effect in
141 *cyp19a1b*$^{+/+}$ males (Fig. 2, B and C), significantly shortened the latency to (P = 0.0005) and increased
142 the number of (P = 0.0006) courtship displays in *cyp19a1b*$^{-/-}$ males (Fig. 2, D and E). These results
143 demonstrated that reduced E2 in the brain was the primary cause of the mating defects, indicating a
144 pivotal role of neuroestrogens in male mating behavior. In contrast, E2 treatment was not effective in
145 restoring aggression in *cyp19a1b*$^{-/-}$ males (Fig. S2A). It is possible that the treatment protocol used may
146 have failed to replicate the estrogenic milieu necessary to induce aggression in males.

147 We then considered the mechanism by which neuroestrogens facilitate male-typical behaviors. Our
148 previous study showed that exogenous E2 upregulates the expression of a subtype of AR, Ara, in the
149 medaka brain (19; note that Ara was termed Arb in this reference). We therefore hypothesized that
150 neuroestrogens may facilitate male-typical behaviors by stimulating Ara expression and thereby
151 potentiating 11KT/Ara signaling in the brain. To test this hypothesis, we first examined *ara* expression
152 in the brain of *cyp19a1b*-deficient males by in situ hybridization analysis. Expression of *ara* was
153 significantly lower in *cyp19a1b*$^{-/-}$ males than in *cyp19a1b*$^{+/+}$ males in several preoptic and hypothalamic
154 nuclei that are activated upon mating and/or attack in males (15), including the PPa, pPPp, and NVT (P
155 = 0.0134, 0.0372, and 0.0008, respectively) (Fig. 2, F and G; see Table S1 for abbreviations of brain
156 nuclei). We then performed a similar analysis for the other AR subtype, Arb. Expression of *arb* was
157 significantly lower in *cyp19a1b*$^{-/-}$ than in *cyp19a1b*$^{+/+}$ males in other preoptic and hypothalamic nuclei
158 activated upon mating and/or attack (15), including the PMp, aPPp, and NPT (P = 0.0009, 0.0413, and
159 0.0021, respectively) (Fig. 2, H and I).
160 Next, to determine whether these reductions in *ara* and *arb* expression in *cyp19a1b*$^{-/-}$ males were
161 the result of reduced brain E2, we tested whether E2 treatment could restore the expression of the two
162 genes. In situ hybridization revealed significantly increased *ara* and *arb* expression in most brain nuclei
163 of E2-treated *cyp19a1b*$^{-/-}$ males as compared with vehicle-treated *cyp19a1b*$^{-/-}$ males (similar results
164 were obtained in *cyp19a1b*$^{+/+}$ males) (Fig. 2, J and K; Fig. S2, B and C; Fig. S3), indicating that the
165 decreased *ara* and *arb* expression in *cyp19a1b*$^{-/-}$ males is attributable to reduced E2 levels. Taken
166 together, these results suggest that neuroestrogens elicit male-typical behaviors by stimulating *ara* and
167 *arb* expression in behaviorally relevant brain regions.
168
169 **_cyp19a1b_ deficiency impairs behaviorally relevant signaling pathways downstream of**
170 **ARs**
171 We considered that, if our hypothesis that neuroestrogens facilitate male-typical behaviors by
172 potentiating androgen/AR signaling is correct, then *cyp19a1b*-deficient males should have impaired
173 activation of behaviorally relevant genes that act downstream of ARs. Two neuropeptide genes, *vt*
174 (encoding vasotocin) and *gal* (encoding galanin), have been implicated in male-typical mating and
175 aggressive behaviors in various vertebrates, including medaka and other teleosts (11, 15, 16, 20, 21). In
176 medaka, subsets of neurons in the pNVT and pPMp express *vt* and *gal*, respectively, in an androgen-
177 dependent and hence male-biased manner, and these neurons have been implicated in male-typical
178 behaviors (11, 16, 22). We therefore studied the expression of *vt* and *gal* in the brains of *cyp19a1b*-
179 deficient males.
180 In situ hybridization revealed that, as expected, expression of *vt* in the pNVT of *cyp19a1b*$^{-/-}$ males
181 was significantly reduced to 18% as compared with *cyp19a1b*$^{+/+}$ males (P = 0.0040), a level comparable
182 to that observed in females (Fig. 3, A and B). In contrast, there were no significant differences between
183 genotypes in other brain nuclei (Fig. 3A). Similarly, expression of *gal* in the pPMp of *cyp19a1b*$^{-/-}$ males
184 was reduced to 43% as compared with *cyp19a1b*$^{+/+}$ males (P = 0.0019), while no significant differences

185 were observed in other brain nuclei (Fig. 3, C and D). These results demonstrate that *cyp19a1b*
186 deficiency severely impairs the AR-dependent activation of behaviorally relevant *vt* and *gal* expression,
187 suggesting that neuroestrogens play a substantial role in activating AR signaling.
188

189 **Estrogens directly stimulate the transcription of ARs through ESRs**

190 The above results led us to further explore how neuroestrogens stimulate the expression of *ara* and
191 *arb*. In silico analysis of the medaka *ara* and *arb* loci identified two canonical bipartite estrogen-
192 responsive element (ERE)-like sequences in introns 1 and 2 of *ara* (located at positions +1699 and
193 +2050, respectively, relative to the transcription initiation site) and three in the 5′-flanking region of *arb*
194 (at positions –1272, –2180, and –3327) (Fig. 4, A and B). Thus, neuroestrogens might be able to directly
195 activate the transcription of *ara* and *arb*. To evaluate this likelihood, we conducted in vitro
196 transcriptional activity assays in which luciferase expression was driven by genomic fragments from the
197 *ara* and *arb* loci containing the identified ERE-like sequences.
198 An assay using the *ara* genomic fragment revealed that E2 dose-dependently increased luciferase
199 activity in the presence of any ESR subtype (Esr1, Esr2a, or Esr2b) (Fig. 4C), suggesting that E2 has
200 the ability to directly activate *ara* transcription through ESRs. The introduction of a point mutation into
201 the ERE-like sequence at position +2050 abolished the E2-induced luciferase activity in the presence of
202 any ESR subtype, while mutation at +1699 had no such effect (Fig. 4D). These results suggest that the
203 ERE at position +2050 is responsible for E2-induced activation of *ara* transcription. Because there is
204 evidence that a single ERE half-site is sufficient to confer E2 responsiveness on several genes (23), we
205 performed the assay using *ara* genomic fragments in which a mutation was introduced in either half-site
206 of the ERE at +2050. E2 induction of luciferase activity was abrogated in both cases (Fig. S4A),
207 suggesting that both ERE half-sites are required to confer estrogen responsiveness on *ara*.
208 In the assay using the *arb* genomic fragment, E2 also dose-dependently increased luciferase activity
209 in the presence of any ESR subtype (Fig. 4E). The E2-induced increase was completely abolished by
210 point mutation of the ERE-like sequence at position –3327 in the presence of any ESR subtype (Fig.
211 4F). A similar effect was observed for mutation of the ERE-like sequence at position –1272, but only in
212 the presence of Esr1 and not in the presence of Esr2a or Esr2b (Fig. 4F). These results indicate that E2
213 can directly stimulate *arb* transcription, primarily through the ERE at –3327. Mutations in either half-
214 site of this ERE eliminated induction by E2 in the presence of Esr2a or Esr2b, but not Esr1 (Fig. S4B),
215 suggesting that both ERE half-sites are required to confer estrogen responsiveness on *arb*. Collectively,
216 these experiments suggest that the transcription of *ara* and *arb* can be directly stimulated by estrogens
217 (including neuroestrogens) via the binding of ESRs to canonical bipartite EREs.
218

219 **Neuroestrogens stimulate *ara* and *arb* expression in behaviorally relevant brain**
220 **regions primarily through Esr2a and Esr1, respectively**

221 Next, we investigated whether neuroestrogens can induce *ara* and *arb* expression through ESRs in
222 vivo and, if so, which ESR subtype (Esr1, Esr2a, or Esr2b) mediates this induction. To this end, we

223 examined *ara* and *arb* expression in the brains of males deficient for each ESR subtype by in situ
224 hybridization. We used previously described *esr1*- and *esr2b*-deficient medaka (10, 24) and generated
225 *esr2a*-deficient medaka using the CRISPR (clustered regularly interspaced short palindromic repeats) /
226 Cas9 (CRISPR-associated protein 9) system. Two independent *esr2a*-deficient lines (Δ8 and Δ4) were
227 established (Fig. S5) and used for subsequent behavioral experiments to ensure the reproducibility of
228 the observed phenotypes.

229 In $esr1^{+/+}$ and $esr1^{-/-}$ males, *ara* expression was not significantly different between genotypes in any
230 brain nucleus (Fig. S6A), but *arb* expression was significantly lower in $esr1^{-/-}$ than in $esr1^{+/+}$ males in
231 the PMp and aPPp (P = 0.0111 and 0.0376, respectively) (Fig. 5, A and B). This, together with our
232 observation that *arb* expression in these brain nuclei was also significantly lower in $cyp19a1b^{-/-}$ males
233 (Fig. 2H), suggests that neuroestrogens stimulate *arb* expression in these nuclei primarily through Esr1.
234 In support of this notion, double-label in situ hybridization in the wild-type male brain detected neurons
235 coexpressing *arb* and *esr1* in both the PMp and aPPp (Fig. S6B). In $esr2a^{+/+}$ and $esr2a^{-/-}$ male brains
236 (from the Δ8 line), *ara* expression was significantly lower in $esr2a^{-/-}$ than in $esr2a^{+/+}$ males in the PPa,
237 pPPp, and NVT (P = 0.0359, 0.0430, and 0.0178, respectively) (Fig. 5, C and D), while no significant
238 difference was observed in *arb* expression (Fig. S6C). Considering that *ara* expression in these nuclei
239 was also lower in $cyp19a1b^{-/-}$ males (Fig. 2F), neuroestrogens presumably stimulate *ara* expression in
240 these nuclei mainly through Esr2a. This idea was further supported by double-label in situ hybridization,
241 which detected neurons coexpressing *ara* and *esr2a* in the PPa, pPPp, and NVT of wild-type males (Fig.
242 S6D). Examination of $esr2b^{+/+}$ and $esr2b^{-/-}$ male brains showed significantly lower expression of *ara* in
243 the NAT and higher expression of *arb* in the PPa of $esr2b^{-/-}$ males (Fig. S6, E to H); however, no such
244 changes in expression were observed in $cyp19a1b^{-/-}$ males (Fig. 2, F and H). It therefore seems unlikely
245 that Esr2b mediates the effect of neuroestrogens on AR expression. Collectively, these results suggest
246 that neuroestrogens stimulate *ara* and *arb* expression in behaviorally relevant brain regions primarily
247 through Esr2a and Esr1, respectively.
248

249 **_esr1_- and _esr2a_-deficient males are, respectively, less motivated to mate and less**
250 **aggressive**

251 If Esr1 and Esr2a truly mediate the behavioral effects of neuroestrogens through the activation of
252 AR expression, then *esr1*- and *esr2a*-deficient males should exhibit impaired male-typical behaviors.
253 More specifically, given that Esr1 and Esr2a function to activate the expression of *arb* and *ara*, which
254 are responsible for male mating and aggression, respectively (15), *esr1*- and *esr2a*-deficient males
255 should be less motivated to mate and less aggressive, respectively.

256 To test these ideas, we first evaluated the mating behavior of *esr1*-deficient males using a wild-type
257 female as the stimulus. As expected, $esr1^{-/-}$ males showed a significantly longer latency to initiate
258 followings than $esr1^{+/+}$ males (P = 0.0055) (Fig. S7), suggesting that they are less motivated to mate.
259 This was further confirmed in tests using an *esr2b*-deficient female as the stimulus, where $esr1^{-/-}$ males
260 showed a longer latency to followings and fewer courtship displays than $esr1^{+/+}$ males (P = 0.0426 and

261 0.0039, respectively) (Fig. 5, E to G). In contrast, no deficits were observed in the mating behavior of
262 *esr2a*$^{-/-}$ males toward wild-type females (Fig. S8, A and B). Although *esr2a*$^{-/-}$ males of the Δ8 line
263 showed a shorter latency to followings than their wild-type siblings in tests using a stimulus *esr2b*-
264 deficient female ($P = 0.0146$) (Fig. 5, H to J), this was not reproduced in the Δ4 line (Fig. S8, C and D).
265 We subsequently assessed aggressive behavior and found no defects in *esr1*$^{-/-}$ males (Fig. 5K).
266 Conversely, *esr2a*$^{-/-}$ males exhibited significantly fewer fin displays ($P = 0.0461$ and 0.0293 for Δ8 and
267 Δ4 lines, respectively) and circles ($P = 0.0446$ and 0.1512 for Δ8 and Δ4 lines, respectively) than their
268 wild-type siblings (Fig. 5L; Fig. S8E), suggesting less aggression. Taken together with the previous
269 finding that *esr2b*-deficient males show no deficits in either mating or aggressive behavior (10), these
270 results suggest that neuroestrogens can promote mating with females by stimulating *arb* expression
271 through Esr1 and can increase aggression toward other males by stimulating *ara* expression through
272 Esr2a. Nonetheless, behavioral deficits in *esr1*- and *esr2a*-deficient males were relatively mild as
273 compared with *cyp19a1b*-deficient males (Fig. 1) and *ara*- and *arb*-deficient males (15), suggesting that
274 a compensatory mechanism may exist between ESR subtypes.
275

276 **_cyp19a1b_-deficient females are less receptive to males and instead court other**
277 **females**

278 Finally, we tested the behavioral impact of *cyp19a1b* deficiency in females. Tests of the mating
279 behavior of *cyp19a1b*$^{-/-}$ females revealed that they had significantly longer latencies to receive the first
280 wrapping from the stimulus male ($P = 0.0018$ versus *cyp19a1b*$^{+/+}$, $P = 0.0117$ versus *cyp19a1b*$^{+/-}$) and
281 to spawn ($P = 0.0015$ versus *cyp19a1b*$^{+/+}$) (Fig. 6, A and B). These results are consistent with a recent
282 study in zebrafish (*Danio rerio*) showing that *cyp19a1b*-deficient females are less receptive to male
283 courtship (25). We further found that the number of courtship displays and wrapping attempts from the
284 male was not increased in *cyp19a1b*$^{-/-}$ females (Fig. 6C), despite their reduced receptivity. This suggests
285 that they are not only less receptive to male courtship but may also actively avoid males, depriving them
286 of mating opportunities. We tested this assumption by measuring the distance between fish, which
287 confirmed that *cyp19a1b*$^{-/-}$ females spent significantly less time near males at distances of 10–20 mm
288 ($P = 0.0438$) and 20–30 mm ($P = 0.0002$) as compared with *cyp19a1b*$^{+/+}$ females (Fig. 6D). We therefore
289 explored the possibility that *cyp19a1b*$^{-/-}$ females may develop a stronger sexual preference for females
290 than for males. In tests of the mating behavior between two females, 4 of 10 *cyp19a1b*$^{-/-}$ females
291 exhibited courtship displays toward the stimulus female, while 0 of 9 *cyp19a1b*$^{+/+}$ females did ($P =$
292 0.0396) (Fig. 6, E and F). These results demonstrate that *cyp19a1b*-deficient females, having a slightly
293 female-oriented sexual preference, are less receptive to male courtship and, conversely, court other
294 females.

295 Notably, these behavioral phenotypes of *cyp19a1b*-deficient females, albeit milder, closely resemble
296 those of *esr2b*-deficient females (10). This led us to hypothesize that *cyp19a1b* deficiency prevents
297 female-typical, and induces male-typical, behavioral phenotypes by decreasing estrogen/Esr2b signaling.
298 If correct, *cyp19a1b*-deficient females should be defective in the activation of behaviorally relevant

genes that act downstream of Esr2b. In medaka, subsets of neurons in the Vs/Vp and PMm/PMg express *npba* (encoding neuropeptide B) in an estrogen/Esr2b signaling-dependent and hence female-specific manner, and these neurons have been implicated in female sexual receptivity (10, 26, 27). We therefore examined the expression of *npba* in the brains of *cyp19a1b*-deficient females by in situ hybridization. As expected, *npba* expression in the Vs/Vp and PMm/PMg of *cyp19a1b*$^{-/-}$ females was significantly reduced to 33% and 38%, respectively, of that of *cyp19a1b*$^{+/+}$ females (Vs/Vp, $P = 0.0386$; PMm/PMg, $P = 0.0461$) (Fig. 6, G to J). Expression of *esr2b* in these brain nuclei is also estrogen-dependent and female-specific (10, 19); therefore, we tested whether it is also attributable to neuroestrogens. In situ hybridization showed no significant differences in *esr2b* expression between *cyp19a1b*$^{+/+}$ and *cyp19a1b*$^{-/-}$ females in the Vs/Vp and PMm/PMg, although significant differences were seen in the VM, NAT, and NVT (Fig. 6K), suggesting that *esr2b* expression in the brain relies on ovarian estrogens and not on neuroestrogens. Taken altogether, our findings indicate that neuroestrogens contribute substantially to the induction of female-typical, and the prevention of male-typical, behaviors in females by activating estrogen/Esr2b signaling.

Discussion

In this study, we found that male medaka deficient for *cyp19a1b* exhibit severely impaired male-typical mating and aggression. This observation was unexpected because the fish had markedly elevated brain levels of 11KT, the primary driver of male-typical behaviors in teleosts (9, 11). These behavioral deficits were rescued by estrogen administration, indicating that reduced levels of neuroestrogens are the primary cause of the observed phenotypes: in other words, neuroestrogens are pivotal for male-typical behaviors in teleosts. This was also unexpected because, unlike in rodents, where the necessity for neuroestrogens has been codified as the "aromatization hypothesis", neuroestrogens have been regarded as dispensable for male behaviors in many vertebrates, including teleosts (7–9). In addition, the rescue of behavioral phenotypes by estrogen administration in adults suggests that in teleosts, unlike in rodents, neuroestrogen activity in adulthood is sufficient for the execution of male-typical behaviors, while that in early in life is not requisite. Thus, while neuroestrogens are necessary for male behaviors in both rodents and teleosts, the life stages at which they exert their behavioral effects probably differ between these species. Brain aromatase activity in teleosts increases with age and, at adulthood, reaches 100–1000 times that in rodents (9, 12). In contrast, brain aromatase activity in rodents reaches its peak during the perinatal period and thereafter declines with age (28). This variation among species may represent the activation of neuroestrogen synthesis at life stages critical for sexual differentiation of behavior that are unique to each species.

Neuroestrogens serve several functions during the process of sexual differentiation of the mouse brain, including the synthesis of prostaglandin PGE2 and the activation of synaptic and neurodevelopmental genes; however, the specific mechanism whereby neuroestrogens affect male behaviors remains obscure (4, 5, 29). Our findings in medaka indicate that neuroestrogens facilitate male-typical behaviors by potentiating androgen/AR signaling in behaviorally relevant brain regions via the direct stimulation of AR transcription. More specifically, they indicate that neuroestrogens (1) promote mating by stimulating the transcription of *arb* in some preoptic and hypothalamus nuclei via Esr1, and (2) increase aggression by stimulating the transcription of *ara* in other preoptic and hypothalamus nuclei through Esr2a. This model of the mechanism underlying neuroestrogen action would explain the apparent contradiction that, in teleosts, androgens per se elicit male behaviors without aromatization, while neuroestrogens are also critical for these behaviors. Our data also indicate that the two AR genes, *ara* and *arb*, are direct downstream targets of neuroestrogens that mediate male behaviors, only a few of which have been identified thus far. In mice, perinatal neuroestrogens increase *Ar* expression in the bed nucleus of the stria terminalis and preoptic area, two brain regions that have been implicated in male behaviors (30). Recent evidence suggests that ESR1 binds to the regulatory genomic region of *Ar* in these brain regions in mice (29). Given these facts, the idea that neuroestrogens enhance androgen/AR signaling by directly stimulating AR transcription may apply to a wide range of species, including rodents.

Consistent with our results, studies in several teleost species have shown that treatment of males

with an aromatase inhibitor reduces their male-typical behaviors (31–33). Conversely, it has been shown in various teleosts, including medaka, that treatment with exogenous estrogens attenuates male behaviors (34–38). A possible explanation for this discrepancy is that estrogens may either stimulate or suppress male-typical behaviors, depending on their concentration. All studies showing the suppressive effects of exogenous estrogens were conducted at doses higher than those used in the present study or at doses mimicking the levels typical of adult females (39). In addition, our previous study in male medaka showed that high doses of exogenous estrogens induce the expression of *esr2b*, which prevents male-typical mating behavior, in behaviorally relevant brain regions (10). Thus, the development of male behaviors may require moderate neuroestrogen levels that are sufficient to induce the expression of *ara* and *arb*, but not *esr2b*, in the underlying neural circuitry. Another possibility, not mutually exclusive, is that endogenous levels of neuroestrogens are sufficient to motivate males to engage in male-typical behaviors, and therefore exogenous estrogens have no further effect. This possibility is supported by the present observation that estrogen treatment facilitated mating behavior in *cyp19a1b*-deficient males but not in their wild-type siblings. Further studies using *cyp19a1b* mutants from different teleost species are needed to explore these possibilities and to determine whether the findings in medaka hold for other teleosts.

We also found that, as compared with males, females have higher brain levels of estrogens, half of which are synthesized locally in the brain (i.e., neuroestrogens). In many brain nuclei of medaka, expression of *ara* and *arb* is comparable between the sexes or at higher levels in females (19), suggesting that neuroestrogens stimulate AR expression in females as well as in males. This raises the issue of why females do not display male-typical behaviors despite such high brain levels of estrogens and active synthesis of neuroestrogens. Possibly, as mentioned above, high estrogen levels in the female brain may suppress male-typical behaviors by promoting the expression of *esr2b*. Another possibility is that females, despite having abundant ARs in the brain, may lack sufficient amounts of androgen to activate them. This seems highly probable because the treatment of female medaka and other teleosts with 11KT as adults readily induces male-typical behaviors, including courtship and aggression (9–11).

We found that *cyp19a1b*-deficient females are less receptive to male courtship, demonstrating that neuroestrogens influence female, as well as male, mating behavior. This finding is notable when considering that, contrary to mammals and birds, estrogens have been deemed unnecessary for female sexual receptivity in teleosts (40). This notion essentially stems from the observation in several teleost species that exogenous prostaglandin PGF2α is sufficient to restore sexual receptivity in females deprived of ovarian secretions by ovariectomy (41–43). However, we recently challenged it by showing that female medaka deficient for *esr2b* are completely unreceptive to males, and thus estrogens play a critical role in female receptivity (10). The present finding provides a likely explanation for this apparent contradiction, namely, that neuroestrogens, rather than or in addition to ovarian-derived circulating estrogens, may function upstream of PGF2α signaling to mediate female receptivity. This scheme potentially applies to other teleost species because a reduction in female receptivity due to *cyp19a1b* deficiency has been also observed in zebrafish (25).

389 We further found that *cyp19a1b*-deficient females court other females. To our knowledge, only a
390 few neuronal genes have been identified whose depletion causes females to display male-typical
391 behaviors in vertebrates. These include *trpc2* (encoding a cation channel crucial for olfactory cue-
392 evoked signaling in the vomeronasal organ) and *dmnt3a* (encoding a methyltransferase responsible for
393 de novo DNA methylation) in mice, and *esr2b* in medaka (10, 44, 45). Importantly, deficiency of
394 *cyp19a1b*, unlike that of *esr2b*, did not completely preclude female-typical mating behavior in females,
395 but caused them to exhibit both male- and female-typical mating behaviors. This observation suggests
396 that, in teleosts, the neural circuits mediating these behaviors coexist in the female brain and may be
397 activated simultaneously in the absence of neuroestrogens. This probably also holds true for the male
398 brain, given that *cyp19a1b*-deficient males also showed impaired, but not completely abolished, male-
399 typical behaviors and were actively courted by *esr2b*-deficient females. It is thus plausible that
400 neuroestrogens are required to prevent the simultaneous activation of neural circuits mediating male-
401 and female-typical behaviors, thereby contributing to the mutually exclusive presentation of these
402 behaviors. Such effects of neuroestrogens are likely to be particularly relevant in teleosts, where many
403 species spontaneously undergo sex reversal and their sexual phenotypes, behavioral or otherwise, are
404 highly labile throughout life (46, 47). This may account for the extremely high levels of aromatase
405 activity in the teleost brain.
406 In summary, we have shown that neuroestrogens promote male-typical behaviors by increasing brain
407 sensitivity to testicular androgens through the stimulation of AR expression. Our findings challenge the
408 prevailing view that neuroestrogens have little effect on male-typical behaviors in species where
409 testicular androgens elicit these behaviors directly without aromatization to neuroestrogens and unveil
410 a previously unappreciated mechanism of neuroestrogen action. Because these species account for the
411 majority of vertebrates, with rodents and some birds being the only known exceptions, the mechanism
412 of neuroestrogen action that we have identified in medaka may be evolutionarily ancient and widely
413 conserved across species.

414 # Materials and Methods

415

416 ## Animals and cell lines

417 Wild-type d-rR strain medaka and mutant medaka deficient for *cyp19a1b* and *esr2a* (generated in
418 this study), *esr1* (24), and *esr2b* (10) were maintained in a recirculating system at 28ºC on a 14/10-hour
419 light/dark cycle. Three or four times a day, they were fed live brine shrimp and dry food (Otohime;
420 Marubeni Nisshin Feed, Tokyo, Japan). Sexually mature adults (2–6 months) were used for experiments,
421 and tissues were consistently sampled 1–5 hours after lights on. In each experiment, siblings raised
422 under the same conditions were used as the comparison group to control for the effects of genetic
423 diversity and environmental variation. All fish were handled in accordance with the guidelines of the
424 Institutional Animal Care and Use Committee of the University of Tokyo.

425 HEK293T and HeLa cells used in this study were confirmed to be mycoplasma-free (Biotherapy
426 Institute of Japan, Tokyo, Japan) and authenticated by short tandem repeat profiling (National Institute
427 of Biomedical Innovation, Osaka, Japan).

428

429 ## Generation of mutant medaka

430 *cyp19a1b*-deficient medaka were generated essentially as previously described (10). In brief, a
431 TILLING library of 5760 chemically mutagenized medaka (14) was screened for mutations in exons 3,
432 4, and 5 of *cyp19a1b* by direct sequencing of PCR-amplified fragments. A founder (ID: 57D05) with a
433 nonsense mutation in exon 4 (K105*) was identified (Fig. S1, A and B) and backcrossed to the wild-
434 type d-rR strain for more than six generations to eliminate background mutations. Heterozygous males
435 and females were intercrossed to generate wild-type, heterozygous, and homozygous siblings. All
436 experimental fish were subjected to genotyping by PCR amplification across the mutation, followed by
437 high-resolution melting (HRM) analysis, using the primers and probe listed in Table S2. HRM analysis
438 was performed on the LightCycler 480 System II (Roche Diagnostics, Basel, Switzerland) using the
439 LCGreen Plus dye (BioFire Defense, Salt Lake City, UT).

440 *esr2a*-deficient medaka were generated by using the CRISPR/Cas9 system. A CRISPR RNA
441 (crRNA) targeting exon 3 of *esr2a* (Fasmac, Kanagawa, Japan) (Fig. S5A) was injected with trans-
442 activating crRNA (Fasmac) and Cas9 protein (Nippon Gene Co. Ltd., Tokyo, Japan) into the cytoplasm
443 of one- or two-cell stage embryos. The resulting fish were screened for germline mutations by
444 outcrossing to wild-type fish and testing progeny for target site mutations by T7 endonuclease I assay
445 (48) and direct sequencing. Two founders were identified that reproducibly yielded progeny carrying
446 frameshift mutations that eliminated the DNA- and ligand-binding domains of Esr2a: one yielded
447 progeny carrying an 8-bp deletion (Δ8); the other yielded progeny carrying a 4-bp deletion (Δ4) (Fig.
448 S5, A and B). The progeny were intercrossed to obtain wild-type, heterozygous, and homozygous
449 siblings. The genotype of each experimental fish was determined by HRM analysis as described above.

450

451 ## Measurement of sex steroid levels

452 Brain and peripheral levels of sex steroids were determined by enzyme-linked immunosorbent assay
453 (ELISA) (10). Total lipids were extracted from the brain and peripheral tissues (from the caudal half) of
454 *cyp19a1b*$^{+/+}$, *cyp19a1b*$^{+/-}$, and *cyp19a1b*$^{-/-}$ males and females with chloroform/methanol (2:1, v/v) and
455 purified on a Sep-Pak C18 Plus Light Cartridge (Waters Corporation, Milford, MA). Tissue levels of
456 E2, testosterone, and 11KT were measured by using Estradiol, Testosterone, and 11-Keto Testosterone
457 ELISA kits, respectively (Cayman Chemical Company, Ann Arbor, MI).
458
459 **Mating behavior test**
460 Mating behavior was tested essentially as previously described (27). In brief, on the day before
461 behavioral testing, each focal fish (*cyp19a1b*-, *esr1*-, and *esr2a*-deficient lines) was placed with a
462 stimulus fish (wild-type females in the tests shown in Fig. 1, C and D, Fig. 6, E and F, Fig. S7, and Fig.
463 S8, A and B; *esr2b*-deficient females in Fig. 1, E to H, Fig. 2, A to E, Fig. 5, E to J, and Fig. S8, C and
464 D; wild-type males in Fig. 6, A to C) in a 2-liter rectangular tank with a perforated transparent partition
465 separating them. The set-up was modified for E2-treated males, which were kept on E2 treatment and
466 not introduced to the test tanks until the day of testing. The partition was removed 1 hour after lights on,
467 and fish were allowed to interact for 30 min while their behavior was recorded with a digital video
468 camera (HC-V360MS, HC-VX985M, or HC-W870M; Panasonic Corporation, Osaka, Japan). The first
469 15 min of the recording was used to calculate the latency to the first following, courtship display,
470 wrapping, and spawning. The period of interaction/recording was extended to 2 hours in tests of
471 courtship displays received from the stimulus *esr2b*-deficient female and in tests of mating behavior
472 between females, because they take longer to initiate courtship (10). In tests using an *esr2b*-deficient
473 female as the stimulus fish, where the latency to spawn could not be calculated because these fish were
474 unreceptive to males and did not spawn, the sexual motivation of the focal fish was instead assessed by
475 counting the number of courtship displays and wrapping attempts in 30 min. The number of these mating
476 acts was also counted in tests to evaluate the receptivity of females. In tests of mating behavior between
477 two females, the stimulus female was marked with a small notch in the caudal fin to distinguish it from
478 the focal female.
479
480 **Aggressive behavior test**
481 To test male–male aggressive behavior (16), four males of the same genotype (*cyp19a1b*-, *esr1*-,
482 and *esr2a*-deficient lines) that were unfamiliar with one another were placed together in a test tank 1
483 hour after lights on. After 1 min of acclimation to the tank, fish were allowed to interact for 15 min
484 while their behavior was video-recorded as described above. The total number of each aggressive act
485 (chase, fin display, circle, strike, and bite) displayed by the four males in the tank was counted manually
486 from the video recordings.
487
488 **E2 treatment**
489 *cyp19a1b*$^{+/+}$ and *cyp19a1b*$^{-/-}$ males were treated with 1 ng/ml of E2 (Fujifilm Wako Pure Chemical,

490 Osaka, Japan) or vehicle (ethanol) alone by immersion in water for 4 days. The mating and aggressive
491 behaviors of males before and after E2 treatment were evaluated as described above. The expression of
492 *ara* and *arb* in the brain of E2- and vehicle-treated males was investigated by single-label in situ
493 hybridization as described below.
494

495 **Single-label in situ hybridization**

496 Digoxigenin (DIG)-labeled cRNA probes were generated by in vitro transcription using DIG RNA
497 Labeling Mix (Roche Diagnostics), T7 RNA polymerase (Roche Diagnostics), and the following cDNA
498 fragments: *ara*, nucleotide 16–1030 of GenBank NM_001122911 (1015 bp); *arb*, 53–1233 of
499 NM_001104681 (1181 bp); *vt*, 1–845 of NM_001278891 (845 bp); *gal*, 5–533 of LC532140 (529 bp);
500 *npba*, 1–645 of NM_001308979 (645 bp); and *esr2b*, 2080–3288 of XM_020713365 (1209 bp).
501 Single-label in situ hybridization was essentially done as described (49). In brief, brains dissected
502 from males and females of the *cyp19a1b*-deficient line (analysis of *ara*, *arb*, *vt*, *gal*, *npba*, and *esr2b*)
503 and males of the *esr1*-, *esr2a*-, and *esr2b*-deficient lines (analysis of *ara* and *arb*) were fixed in 4%
504 paraformaldehyde and embedded in paraffin. Serial coronal sections of 10-µm thickness were
505 hybridized with a DIG-labeled probe. Hybridization signal was detected with anti-DIG conjugated to
506 alkaline phosphatase (RRID: AB_514497; Roche Diagnostics) and visualized using 5-bromo-4-chloro-
507 3-indolyl phosphate/nitro blue tetrazolium substrate (Roche Diagnostics). After color development for
508 15 min (*gal*), 40 min (*npba*), 2 hours (*vt*), or overnight (*ara*, *arb*, and *esr2b*), sections were imaged using
509 a VS120 virtual slide microscope (Olympus, Tokyo, Japan), and the total area of signal in each brain
510 nucleus was calculated using Olyvia software (Olympus). Medaka brain atlases (50, 51) were used to
511 identify brain nuclei.
512

513 **Transcriptional activity assay**

514 Each full-length coding region of medaka Esr1 (GenBank XM_020714493), Esr2a
515 (NM_001104702), and Esr2b (XM_020713365) cDNA was amplified by PCR and inserted into the
516 expression vector pcDNA3.1/V5-His-TOPO (Thermo Fisher Scientific, Waltham, MA). Each
517 nucleotide sequence of the 5′-flanking region of *ara* and *arb* was retrieved from the Ensembl medaka
518 genome assembly and analyzed for potential canonical ERE-like sequences using Jaspar (version
519 5.0_alpha) and Match (public version 1.0) with default settings. No ERE-like sequence was detected in
520 *ara*; therefore, the gene body and 3′-flanking region were also analyzed in this case. The transcription
521 initiation site for *ara* and *arb* was determined based on an expressed sequence tag clone deposited in
522 National BioResource Project (NBRP) Medaka (olova36n18) and GenBank NM_001104681,
523 respectively. Medaka bacterial artificial chromosome (BAC) clones containing the *ara* (clone ID: ola1-
524 111G01) and *arb* (ola1-192H15) loci were obtained from NBRP Medaka. A 4530-bp genomic DNA
525 fragment upstream of *ara* exon 3 (comprising 2330 bp of the 5′-flanking region, exon 1, intron 1, exon
526 2, intron 2, and the first 32 bp of exon 3) was amplified by PCR from the BAC clone, fused to a P2A
527 self-cleaving peptide sequence (52) at the 3′ end, and inserted into the NheI site of the luciferase reporter

528 vector pGL4.10 (Promega, Madison, WI). Similarly, a 3995-bp fragment upstream of the first
529 methionine codon of *arb* (comprising 3815 bp of the 5′-flanking region and 180 bp of exon1) was PCR-
530 amplified and inserted into pGL4.10. The resulting constructs were transiently transfected into
531 HEK293T (*ara*) or HeLa (*arb*) cells, together with an internal control vector pGL4.74 (Promega) and
532 the Esr1, Esr2a, or Esr2b expression construct using Lipofectamine LTX (Thermo Fisher Scientific).
533 Six hours after transfection, cells were incubated for 18 hours without and with E2 at doses of 10^{-11} M,
534 10^{-9} M, and 10^{-7} M in Dulbecco's modified Eagle's medium (phenol red-free) containing 5%
535 charcoal/dextran-stripped fetal bovine serum (Cytiva, Marlborough, MA). Luciferase activity was
536 determined using the Dual-Luciferase Reporter Assay System (Promega) on the GloMax 20/20n
537 Luminometer (Promega). All assays were conducted in duplicate or triplicate and repeated
538 independently three times.
539 Further assays were performed with luciferase reporter constructs carrying point mutations in the
540 ERE-like sequences to identify the ERE responsible for E2 induction of *ara* and *arb* transcription. Each
541 half-site of the responsible ERE-like sequence was mutated into a HindIII recognition site using the
542 PrimeSTAR Mutagenesis Basal Kit (Takara Bio, Shiga, Japan). Transcriptional activity assays with
543 these constructs were done as described above, except that a single dose of E2 (10^{-7} M) was used.
544

545 **Double-label in situ hybridization**

546 DIG-labeled cRNA probes for *ara* and *arb* were prepared as described above. Fluorescein-labeled
547 cRNA probes for *esr1* and *esr2a* were generated by in vitro transcription using Fluorescein RNA
548 Labeling Mix (Roche Diagnostics), SP6 or T7 RNA polymerase (Roche Diagnostics), and the following
549 cDNA fragments: *esr1*, nucleotides 1694–2781 of XM_020714493 (1088 bp); *esr2a*, 1838–2276 of
550 NM_001104702 plus 763 bp of 3′-untranslated sequence derived from the Ensembl medaka genome
551 assembly (439 bp).
552 Double-label in situ hybridization was done as described previously (24), with minor modifications.
553 In brief, brains dissected from wild-type males were fixed in 4% paraformaldehyde, embedded in
554 paraffin, and coronally sectioned at 10-µm thickness. Sections were hybridized simultaneously with the
555 DIG-labeled *ara* or *arb* probe and fluorescein-labeled *esr1* or *esr2a* probe. DIG was detected with a
556 mouse anti-DIG antibody (RRID: AB_304362; Abcam, Cambridge, UK) and visualized using the Alexa
557 Fluor 555 Tyramide SuperBoost Kit, goat anti-mouse IgG (Thermo Fisher Scientific); fluorescein was
558 detected with an anti-fluorescein antibody conjugated to horseradish peroxidase (RRID: AB_2737388;
559 PerkinElmer, Waltham, MA) and visualized using the TSA Plus Fluorescein System (PerkinElmer).
560 Cell nuclei were counterstained with DAPI. Fluorescent images were acquired with a Leica TCS SP8
561 confocal laser scanning microscope (Leica Microsystems, Wetzlar, Germany) and the following
562 excitation/emission wavelengths: 552/620–700 nm (Alexa Fluor 555), 488/495–545 nm (fluorescein),
563 and 405/410–480 nm (DAPI).
564

565 **Measurement of spatial distances between fish**

566 The distance between the two fish in the test tank was measured as described elsewhere (10). On the
567 day preceding measurement, each focal female (*cyp19a1b*-deficient line) and a stimulus wild-type male
568 were placed together in a 2-liter rectangular tank with a perforated transparent partition separating them.
569 On the following day after lights on, the fish were transferred to a 25-cm (i,d,) cylindrical test tank
570 containing 1.8 L of dechlorinated tap water with a transparent partition separating them. One hour after
571 lights on, the partition was removed and the behavior of the fish was video-recorded for 10 min.
572 Distances between fish were calculated by using UMA Tracker (53).
573
574 **Statistical analysis**
575 All quantitative data were expressed as mean ± standard error of the mean (SEM). On graphs,
576 individual data points were plotted to indicate the underlying distribution. Behavioral time-series data
577 were analyzed using Kaplan–Meier plots with the inclusion of fish that did not exhibit the given act
578 within the test period.
579 Statistical analyses were done using GraphPad Prism (GraphPad Software, San Diego, CA). Data
580 between two groups were compared using unpaired two-tailed Student's *t* test. Welch's correction was
581 applied if the *F* test indicated that the variance between groups was significantly different. The
582 Bonferroni–Dunn correction was applied for multiple comparisons between two groups. To compare
583 data among more than two groups, one-way analysis of variance (ANOVA) was performed, followed
584 by either Bonferroni's (comparisons among experimental groups) or Dunnett's (comparisons between
585 control and experimental groups) post hoc test. If the Brown-Forsythe test indicated a significant
586 difference in variance across groups, the data were instead analyzed using the non-parametric Kruskal–
587 Wallis test, followed by Dunn's post hoc test. Differences between Kaplan–Meier curves were tested
588 for significance using the Gehan–Breslow–Wilcoxon test (with Bonferroni's correction for more than
589 two comparisons). Fish that spawned without any courtship display were excluded from the analysis of
590 courtship display because it was not appropriate to treat them either as fish that did not perform courtship
591 displays within the test duration or as fish that performed the first courtship display 0 seconds before
592 spawning. All data points were included in the analyses and no outliers were defined.

Acknowledgments

We thank NBRP Medaka for providing the BAC clones, managing the TILLING library, and performing artificial insemination; Dr. Yoshihito Taniguchi for constructing the TILLING library; Dr. Masatoshi Nakamoto for recovering the *cyp19a1b* mutant allele; Akira Hirata, Kaoru Furukawa, Tomiko Iba, and Ayu Kuwakubo for assistance with medaka husbandry. This work was supported by the Ministry of Education, Culture, Sports, Science, and Technology (MEXT), Japan (17H06429 to KOk), the Japan Society for the Promotion of Science (JSPS) (21J20634 to YNi and 23H02305 to KOk), and Regional Fish Institute (Get-Research Grant to KOk).

References

1. N. Zilkha, Y. Sofer, Y. Kashash, T. Kimchi, The social network: neural control of sex differences in reproductive behaviors, motivation, and response to social isolation. *Curr. Opin. Neurobiol.* **68**, 137–151 (2021).
2. S. Ogawa, S. Tsukahara, E. Choleris, N. Vasudevan, Estrogenic regulation of social behavior and sexually dimorphic brain formation. *Neurosci. Biobehav. Rev.* **110**, 46–59 (2020).
3. S. Tsukahara, M. Morishita, Sexually dimorphic formation of the preoptic area and the bed nucleus of the stria terminalis by neuroestrogens. *Front. Neurosci.* **14**, 797 (2020).
4. M. M. McCarthy, Neural control of sexually dimorphic social behavior: connecting development to adulthood. *Annu. Rev. Neurosci.* **46**, 321–339 (2023).
5. M. M. McCarthy, B. M. Nugent, K. M. Lenz, Neuroimmunology and neuroepigenetics in the establishment of sex differences in the brain. *Nat. Rev. Neurosci.* **18**, 471–484 (2017).
6. J. Balthazart, New concepts in the study of the sexual differentiation and activation of reproductive behavior, a personal view. *Front. Neuroendocrinol.* **55**, 100785 (2019).
7. J. Thornton, J. L. Zehr, M. D. Loose, Effects of prenatal androgens on rhesus monkeys: a model system to explore the organizational hypothesis in primates. *Horm. Behav.* **55**, 633–645 (2009).
8. J. Bakker, The role of steroid hormones in the sexual differentiation of the human brain. *J. Neuroendocrinol.* **34**, e13050 (2022).
9. K. Okubo, Y. Nishiike, T. Fleming, Y. Kikuchi, T. Hiraki-Kajiyama, "Sex steroid regulation of male- and female-typical mating behaviors in teleost fish" in *Spectrum of Sex*, M. Tanaka, M. Tachibana, Eds. (Springer Nature, 2022), pp. 111–133.
10. Y. Nishiike, D. Miyazoe, R. Togawa, K. Yokoyama, K. Nakasone, M. Miyata, Y. Kikuchi, Y. Kamei, T. Todo, T. Ishikawa-Fujiwara, K. Ohno, T. Usami, Y. Nagahama, K. Okubo, Estrogen receptor 2b is the major determinant of sex-typical mating behavior and sexual preference in medaka. *Curr. Biol.* **31**, 1699–1710.e6 (2021).
11. Y. Kawabata-Sakata, S. Kanda, K. Okubo, Male-specific vasotocin expression in the medaka tuberal hypothalamus: androgen dependence and probable role in aggression. *Mol. Cell. Endocrinol.* **580**, 112101 (2024).
12. N. Diotel, T. D. Charlier, C. Lefebvre d'Hellencourt, D. Couret, V. L. Trudeau, J. C. Nicolau, O. Meilhac, O. Kah, E. Pellegrini, Steroid transport, local synthesis, and signaling within the brain: roles in neurogenesis, neuroprotection, and sexual behaviors. *Front. Neurosci.* **12**, 84 (2018).
13. Y. Nagahama, T. Chakraborty, B. Paul-Prasanth, K. Ohta, M. Nakamura, Sex determination, gonadal sex differentiation, and plasticity in vertebrate species. *Physiol. Rev.* **101**, 1237–1308 (2021).
14. Y. Taniguchi, S. Takeda, M. Furutani-Seiki, Y. Kamei, T. Todo, T. Sasado, T. Deguchi, H. Kondoh, J. Mudde, M. Yamazoe, M. Hidaka, H. Mitani, A. Toyoda, Y. Sakaki, R. H. A. Plasterk, E. Cuppen, Generation of medaka gene knockout models by target-selected mutagenesis. *Genome Biol.* **7**,

R116 (2006).
15. Y. Nishiike, K. Okubo, The decision of male medaka to mate or fight depends on two complementary androgen signaling pathways. *bioRxiv* doi: 10.1101/2024.01.10.574747 (2024).
16. J. Yamashita, A. Takeuchi, K. Hosono, T. Fleming, Y. Nagahama, K. Okubo, Male-predominant galanin mediates androgen-dependent aggressive chases in medaka. *eLife* **9**, e59470 (2020).
17. X. Zhang, Q. Min, M. Li, X. Liu, M. Li, D. Wang, Mutation of *cyp19a1b* results in sterile males due to efferent duct obstruction in Nile tilapia. *Mol. Reprod. Dev.* **86**, 1224–1235 (2019).
18. Y. Ogino, S. Ansai, E. Watanabe, M. Yasugi, Y. Katayama, H. Sakamoto, K. Okamoto, K. Okubo, Y. Yamamoto, I. Hara, T. Yamazaki, A. Kato, Y. Kamei, K. Naruse, K. Ohta, H. Ogino, T. Sakamoto, S. Miyagawa, T. Sato, G. Yamada, M. E. Baker, T. Iguchi, Evolutionary differentiation of androgen receptor is responsible for sexual characteristic development in a teleost fish. *Nat. Commun.* **14**, 1428 (2023).
19. T. Hiraki, A. Takeuchi, T. Tsumaki, B. Zempo, S. Kanda, Y. Oka, Y. Nagahama, K. Okubo, Female-specific target sites for both oestrogen and androgen in the teleost brain. *Proc. R. Soc. B* **279**, 5014–5023 (2012).
20. S. Yokoi, T. Okuyama, Y. Kamei, K. Naruse, Y. Taniguchi, S. Ansai, M. Kinoshita, L. J. Young, N. Takemori, T. Kubo, H. Takeuchi, An essential role of the arginine vasotocin system in mate-guarding behaviors in triadic relationships of medaka fish (*Oryzias latipes*). *PLoS Genet.* **11**, e1005009 (2015).
21. J. A. Tripp, I. Salas-Allende, A. Makowski, A. H. Bass, Mating behavioral function of preoptic galanin neurons is shared between fish with alternative male reproductive tactics and tetrapods. *J. Neurosci.* **40**, 1549–1559 (2020).
22. Y. Kawabata, T. Hiraki, A. Takeuchi, K. Okubo, Sex differences in the expression of vasotocin/isotocin, gonadotropin-releasing hormone, and tyrosine and tryptophan hydroxylase family genes in the medaka brain. *Neuroscience* **218**, 65–77 (2012).
23. C. M. Klinge, Estrogen receptor interaction with estrogen response elements. *Nucleic Acids Res.* **29**, 2905–2919 (2001).
24. T. Fleming, M. Tachizawa, Y. Nishiike, A. Koiwa, Y. Homan, K. Okubo, Estrogen-dependent expression and function of secretogranin 2a in female-specific peptidergic neurons. *PNAS Nexus* **2**, pgad413 (2023).
25. K. Shaw, M. Therrien, C. Lu, X. Liu, V. L. Trudeau, Mutation of brain aromatase disrupts spawning behavior and reproductive health in female zebrafish. *Front. Endocrinol.* **14**, 1225199 (2023).
26. T. Hiraki, K. Nakasone, K. Hosono, Y. Kawabata, Y. Nagahama, K. Okubo, Neuropeptide B is female-specifically expressed in the telencephalic and preoptic nuclei of the medaka brain. *Endocrinology* **155**, 1021–1032 (2014).
27. T. Hiraki-Kajiyama, J. Yamashita, K. Yokoyama, Y. Kikuchi, M. Nakajo, D. Miyazoe, Y. Nishiike, K. Ishikawa, K. Hosono, Y. Kawabata-Sakata, S. Ansai, M. Kinoshita, Y. Nagahama, K. Okubo, Neuropeptide B mediates female sexual receptivity in medaka fish, acting in a female-specific but

reversible manner. *eLife* **8**, e39495 (2019).

28. E. D. Lephart, A review of brain aromatase cytochrome P450. *Brain Res. Rev.* **22**, 1–26 (1996).
29. B. Gegenhuber, M. V. Wu, R. Bronstein, J. Tollkuhn, Gene regulation by gonadal hormone receptors underlies brain sex differences. *Nature* **606**, 153–159 (2022).
30. S. A. Juntti, J. Tollkuhn, M. V. Wu, E. J. Fraser, T. Soderborg, S. Tan, S.-I. Honda, N. Harada, N. M. Shah, The androgen receptor governs the execution, but not programming, of male sexual and territorial behaviors. *Neuron* **66**, 260–272 (2010).
31. S. L. E. Hallgren, M. Linderoth, K. H. Olsén, Inhibition of cytochrome p450 brain aromatase reduces two male specific sexual behaviours in the male Endler guppy (*Poecilia reticulata*). *Gen. Comp. Endocrinol.* **147**, 323–328 (2006).
32. L. S. Huffman, L. A. O'Connell, H. A. Hofmann, Aromatase regulates aggression in the African cichlid fish *Astatotilapia burtoni*. *Physiol. Behav.* **112**, 77–83 (2013).
33. C. Jalabert, L. Quintana, P. Pessina, A. Silva, Extra-gonadal steroids modulate non-breeding territorial aggression in weakly electric fish. *Horm. Behav.* **72**, 60–67 (2015).
34. M. Bayley, J. R. Nielsen, E. Baatrup, Guppy sexual behavior as an effect biomarker of estrogen mimics. *Ecotoxicol. Environ. Saf.* **43**, 68–73 (1999).
35. A. M. Bell, Effects of an endocrine disrupter on courtship and aggressive behaviour of male three-spined stickleback, *Gasterosteus aculeatus*. *Anim. Behav.* **62**, 775–780 (2001).
36. R. Bjerselius, K. Lundstedt-Enkel, H. Olsén, I. Mayer, K. Dimberg, Male goldfish reproductive behaviour and physiology are severely affected by exogenous exposure to 17β-estradiol. *Aquat. Toxicol.* **53**, 139–152 (2001).
37. Y. Oshima, I. J. Kang, M. Kobayashi, K. Nakayama, N. Imada, T. Honjo, Suppression of sexual behavior in male Japanese medaka (*Oryzias latipes*) exposed to 17β-estradiol. *Chemosphere* **50**, 429–436 (2003).
38. D. Martinović, W. T. Hogarth, R. E. Jones, P. W. Sorensen, Environmental estrogens suppress hormones, behavior, and reproductive fitness in male fathead minnows. *Environ. Toxicol. Chem.* **26**, 271–278 (2007).
39. D. Kayo, Y. Oka, S. Kanda, Examination of methods for manipulating serum 17β-Estradiol (E2) levels by analysis of blood E2 concentration in medaka (*Oryzias latipes*). Gen Comp. Endocrinol. **285**, 113272 (2020).
40. A. Munakata, M. Kobayashi, Endocrine control of sexual behavior in teleost fish. *Gen. Comp. Endocrinol.* **165**, 456–468 (2010).
41. N. E. Stacey, Effects of indomethacin and prostaglandins on the spawning behaviour of female goldfish. *Prostaglandins* **12**, 113–126 (1976).
42. M. Kobayashi, N. Stacey, Prostaglandin-induced female spawning behavior in goldfish (*Carassius auratus*) appears independent of ovarian influence. *Horm. Behav.* **27**, 38–55 (1993).
43. S. A. Juntti, A. T. Hilliard, K. R. Kent, A. Kumar, A. Nguyen, M. A. Jimenez, J. L. Loveland, P. Mourrain, R. D. Fernald, A neural basis for control of cichlid female reproductive behavior by

716 prostaglandin F2α. *Curr. Biol.* **26**, 943–949 (2016).
717 44. T. Kimchi, J. Xu, C. Dulac, A functional circuit underlying male sexual behaviour in the female
718 mouse brain. *Nature* **448**, 1009–1014 (2007).
719 45. B. M. Nugent, C. L. Wright, A. C. Shetty, G. E. Hodes, K. M. Lenz, A. Mahurkar, S. J. Russo, S.
720 E. Devine, M. M. McCarthy, Brain feminization requires active repression of masculinization via
721 DNA methylation. *Nat. Neurosci.* **18**, 690–697 (2015).
722 46. B. Capel, Vertebrate sex determination: evolutionary plasticity of a fundamental switch. *Nat. Rev.*
723 *Genet.* **18**, 675–689 (2017).
724 47. H. Liu, E. V. Todd, P. M. Lokman, M. S. Lamm, J. R. Godwin, N. J. Gemmell, Sexual plasticity: a
725 fishy tale. *Mol. Reprod. Dev.* **84**, 171–194 (2017).
726 48. H. J. Kim, H. J. Lee, H. Kim, S. W. Cho, J.-S. Kim, Targeted genome editing in human cells with
727 zinc finger nucleases constructed via modular assembly. *Genome Res.* **19**, 1279–1288 (2009).
728 49. Y. Kawabata-Sakata, Y. Nishiike, T. Fleming, Y. Kikuchi, K. Okubo, Androgen-dependent sexual
729 dimorphism in pituitary tryptophan hydroxylase expression: relevance to sex differences in
730 pituitary hormones. *Proc. R. Soc. B* **287**, 20200713 (2020).
731 50. R. Anken, F. Bourrat, *Brain Atlas of the Medaka fish* (INRA Editions, 1998).
732 51. Y. Ishikawa, M. Yoshimoto, H. Ito, A brain atlas of a wild-type inbred strain of the medaka, *Oryzias*
733 *latipes*. *Fish Biol. J. Medaka* **10**, 1–26 (1999).
734 52. J. H. Kim, S. R. Lee, L. H. Li, H. J. Park, J. H. Park, K. Y. Lee, M. K. Kim, B. A. Shin, S. Y. Choi,
735 High cleavage efficiency of a 2A peptide derived from porcine teschovirus-1 in human cell lines,
736 zebrafish and mice. *PLoS One* **6**, e18556 (2011).
737 53. O. Yamanaka, R. Takeuchi, UMATracker: an intuitive image-based tracking platform. *J. Exp. Biol.*
738 **221**, jeb182469 (2018).

Figures

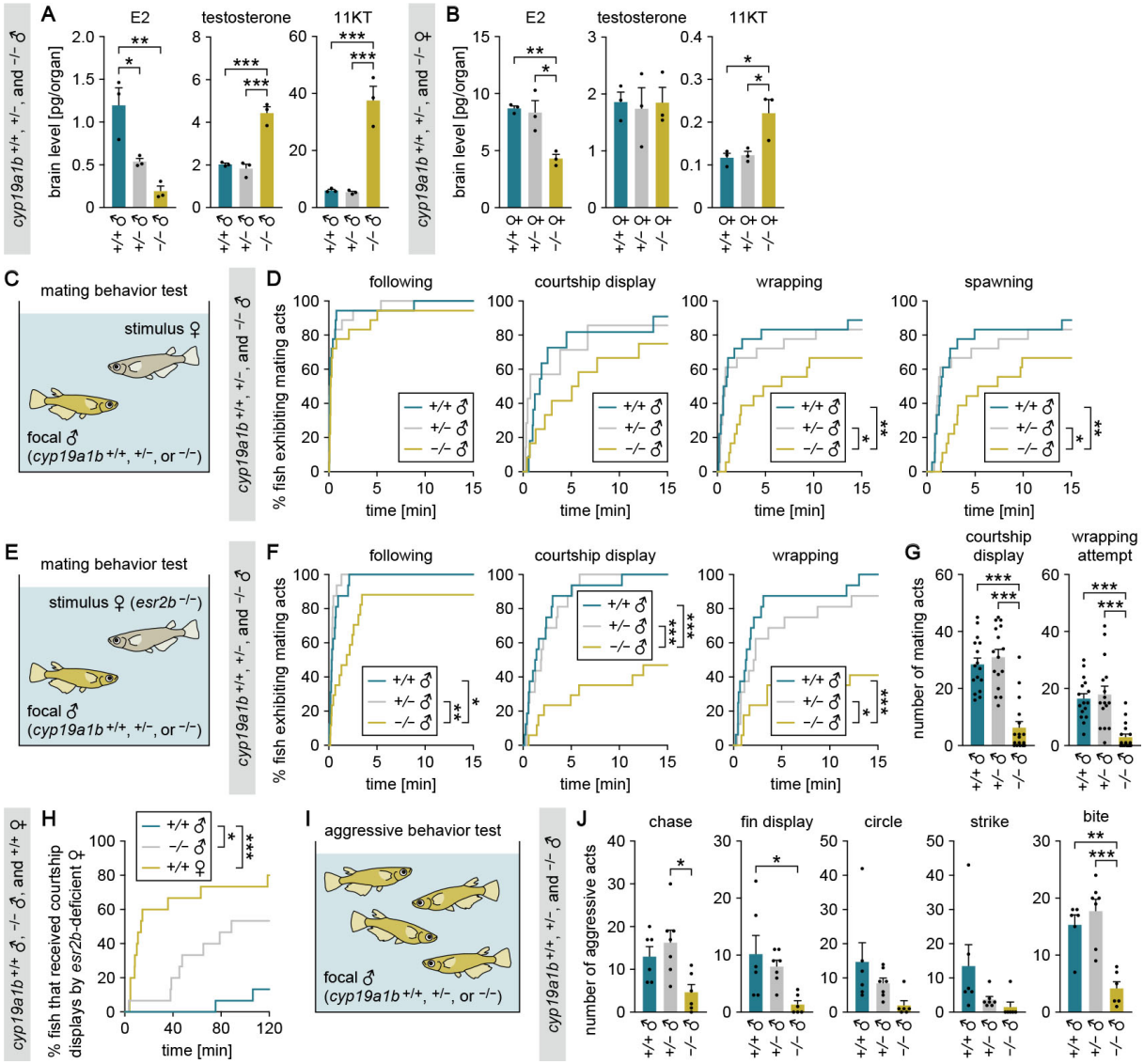

Fig. 1 *cyp19a1b*-deficient males exhibit severely impaired male-typical mating and aggressive behaviors.

(**A** and **B**) Levels of E2, testosterone, and 11KT in the brain of adult *cyp19a1b*$^{+/+}$, *cyp19a1b*$^{+/-}$, and *cyp19a1b*$^{-/-}$ males (A) and females (B) (n = 3 per genotype and sex). (**C**) Set-up for testing the mating behavior of *cyp19a1b*$^{+/+}$, *cyp19a1b*$^{+/-}$, and *cyp19a1b*$^{-/-}$ males. (**D**) Latency of *cyp19a1b*$^{+/+}$, *cyp19a1b*$^{+/-}$, and *cyp19a1b*$^{-/-}$ males (n = 18 per genotype) to initiate each mating act toward the stimulus female. (**E**) Set-up for testing mating behavior using an *esr2b*-deficient female as the stimulus. (**F**) Latency of *cyp19a1b*$^{+/+}$, *cyp19a1b*$^{+/-}$, and *cyp19a1b*$^{-/-}$ males (n = 16, 15, and 17, respectively) to initiate each mating act toward the *esr2b*-deficient female. (**G**) Number of each mating act performed. (**H**) Latency of *cyp19a1b*$^{+/+}$ and *cyp19a1b*$^{-/-}$ males and *cyp19a1b*$^{+/+}$ females (n = 15 each) to receive courtship displays from the *esr2b*-deficient female. (**I**) Set-up for testing aggressive behavior among grouped males. (**J**) Total number of each aggressive act observed among *cyp19a1b*$^{+/+}$, *cyp19a1b*$^{+/-}$, or

755 *cyp19a1b*$^{-/-}$ males in the tank (n = 6, 7, and 5, respectively). Statistical differences were assessed by
756 Bonferroni's or Dunn's post hoc test (A, B, G, and J) and Gehan-Breslow-Wilcoxon test with
757 Bonferroni's correction (D, F, and H). Error bars represent SEM. *$P < 0.05$, **$P < 0.01$, ***$P < 0.001$.

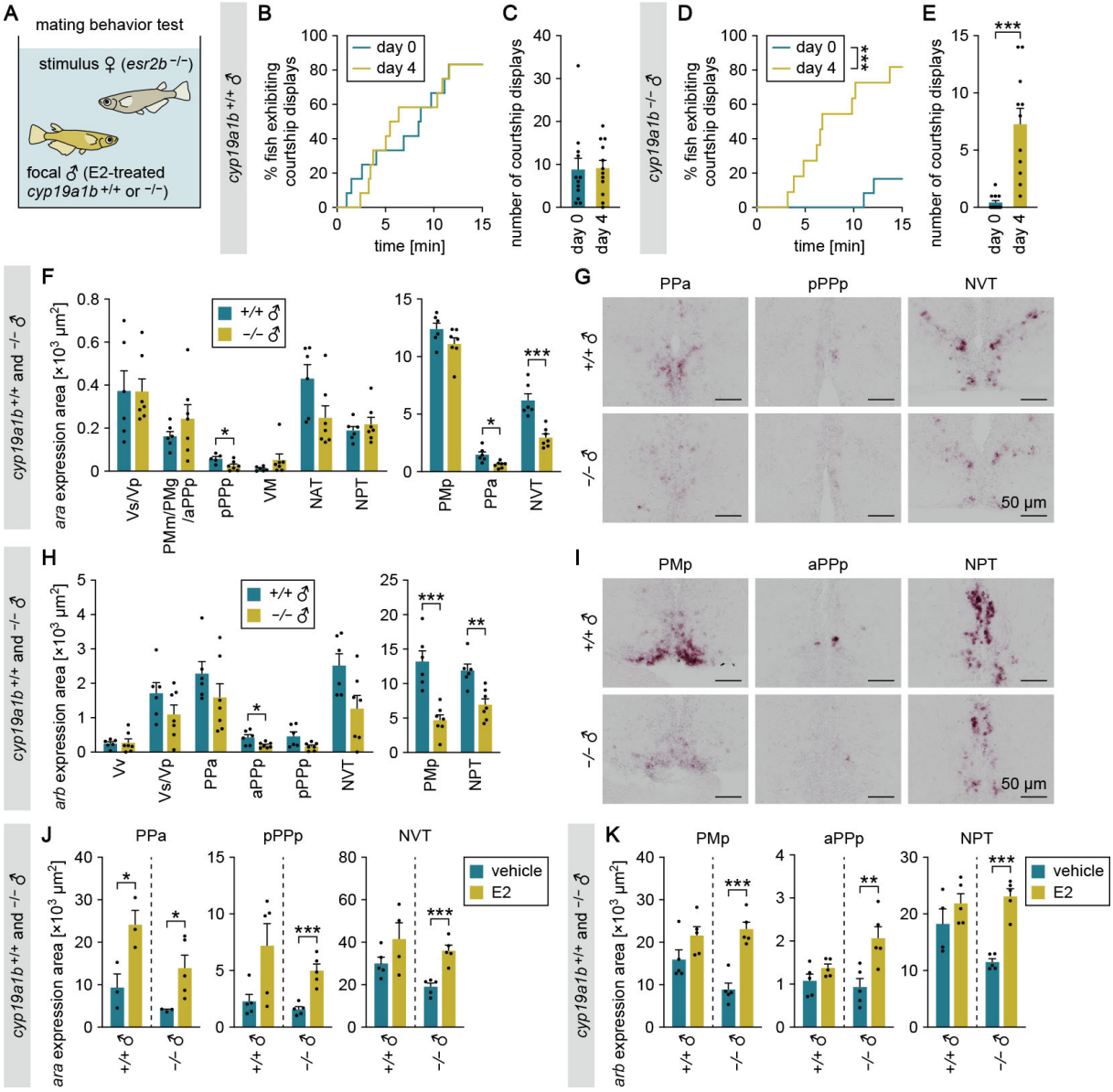

Fig. 2 Neuroestrogens facilitate male-typical behaviors probably by stimulating brain AR expression.

(**A**) Set-up for testing the mating behavior of E2-treated *cyp19a1b*$^{+/+}$ and *cyp19a1b*$^{-/-}$ males. (**B**) Latency of *cyp19a1b*$^{+/+}$ males (n = 12) to initiate courtship displays toward the stimulus female before (day 0) and after (day 4) E2 treatment. (**C**) Number of courtship displays performed by *cyp19a1b*$^{+/+}$ males. (**D**) Latency of *cyp19a1b*$^{-/-}$ males (n = 12) to initiate courtship displays before (day 0) and after (day 4) E2 treatment. (**E**) Number of courtship displays performed by *cyp19a1b*$^{-/-}$ males. (**F**) Total area of *ara* expression signal in each brain nucleus of *cyp19a1b*$^{+/+}$ (n = 6 except for pPPp, where n = 5) and *cyp19a1b*$^{-/-}$ (n = 7) males. The data are displayed in two graphs for visual clarity. (**G**) Representative images of *ara* expression in the PPa, pPPp, and NVT. (**H**) Total area of *arb* expression signal in each brain nucleus of *cyp19a1b*$^{+/+}$ (n = 6) and *cyp19a1b*$^{-/-}$ (n = 7 except for NVT, where n = 6) males. The data are displayed in two graphs for visual clarity. (**I**) Representative images of *arb* expression in the PMp, aPPp, and NPT. (**J**) Total area of *ara* expression signal in the PPa, pPPp, and NVT of *cyp19a1b*$^{+/+}$

773 and *cyp19a1b*$^{-/-}$ males treated with vehicle alone or E2 (n = 5 per group except for NVT of E2-treated
774 *cyp19a1b*$^{+/+}$ males, where n = 4; and PPa of vehicle-treated *cyp19a1b*$^{+/+}$, E2-treated *cyp19a1b*$^{+/+}$, and
775 vehicle-treated *cyp19a1b*$^{-/-}$ males, where n = 3). (**K**) Total area of *arb* expression signal in the PMp,
776 aPPp, and NPT of *cyp19a1b*$^{+/+}$ and *cyp19a1b*$^{-/-}$ males treated with vehicle alone or E2 (n = 5 per group
777 except for NPT of vehicle-treated *cyp19a1b*$^{+/+}$ males, where n = 4). Scale bars represent 50 μm. For
778 abbreviations of brain nuclei, see Table S1. Statistical differences were assessed by Gehan-Breslow-
779 Wilcoxon test (B and D) and unpaired *t* test, with Welch's correction where appropriate (C, E, F, H, J,
780 and K). Error bars represent SEM. *$P < 0.05$, **$P < 0.01$, ***$P < 0.001$.

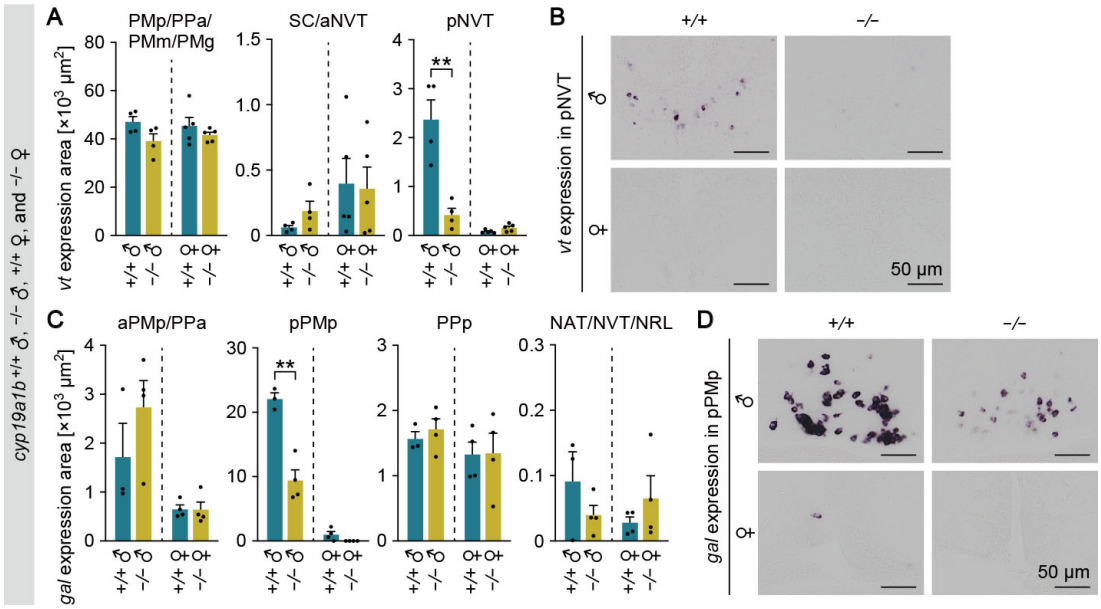

Fig. 3 *cyp19a1b* deficiency impairs behaviorally relevant signaling pathways downstream of ARs.

(**A**) Total area of *vt* expression signal in the PMp/PPa/PMm/PMg, SC/aNVT, and pNVT of *cyp19a1b*$^{+/+}$ and *cyp19a1b*$^{-/-}$ males and females (n = 4 and 5 per genotype for males and females, respectively). (**B**) Representative images of *vt* expression in the pNVT. (**C**) Total area of *gal* expression signal in the aPMp/PPa, pPMp, PPp, and NAT/NVT/NRL of *cyp19a1b*$^{+/+}$ and *cyp19a1b*$^{-/-}$ males and females (n = 4 except for *cyp19a1b*$^{+/+}$ males, where n = 3). (**D**) Representative images of *gal* expression in the pPMp. Scale bars represent 50 µm. For abbreviations of brain nuclei, see Table S1. Statistical differences were assessed by unpaired *t* test, with Welch's correction where appropriate (A and C). Error bars represent SEM. $^{**}P < 0.01$.

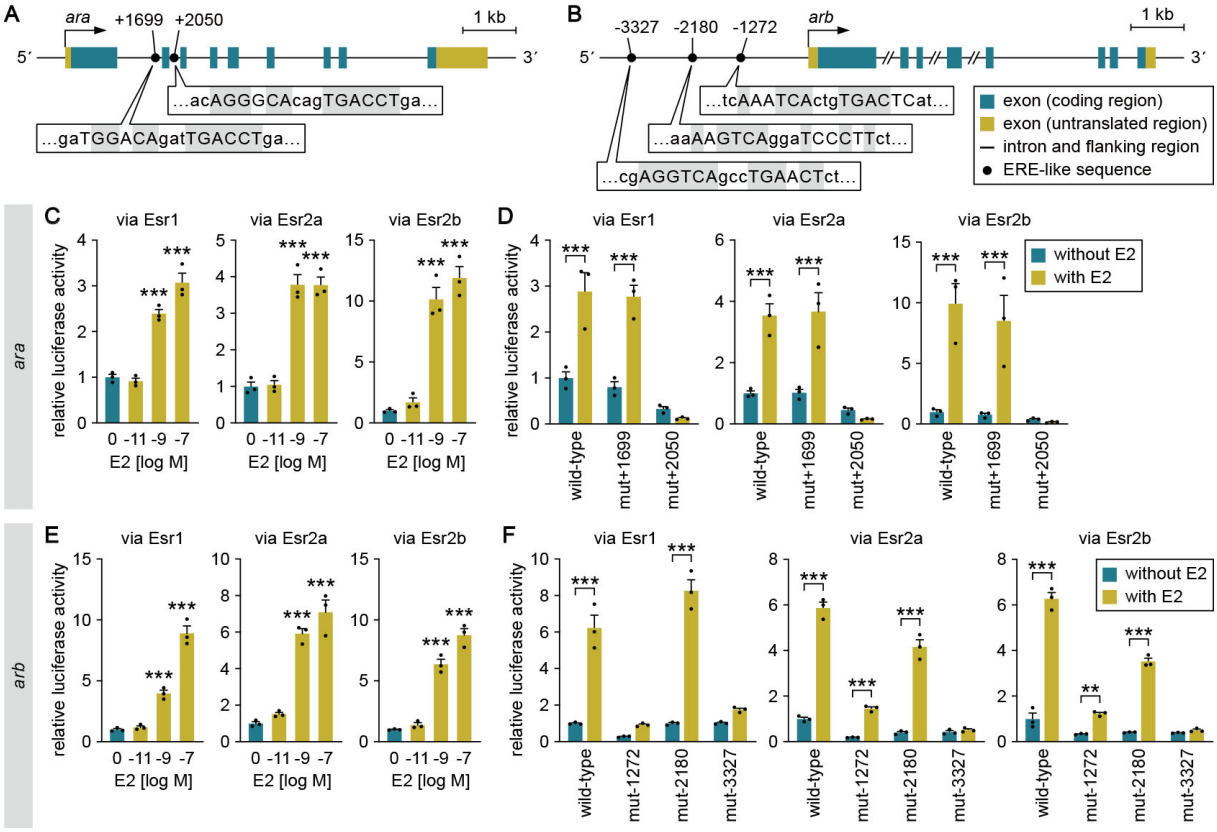

Fig. 4 Estrogens directly stimulate the transcription of ARs through ESRs.

(**A** and **B**) Schematic of *ara* (A) and *arb* (B) loci showing the location of the canonical bipartite ERE-like sequences. Bent arrows mark the transcription initiation sites. Nucleotides of the ERE-like sequences are denoted by capital letters, and those identical to the consensus ERE (AGGTCAnnnTGACCT) are gray-shaded. (**C**) Ability of E2 to directly activate *ara* transcription. Cultured cells were transfected with a luciferase reporter construct containing a genomic fragment upstream of exon 3 of *ara*, together with an Esr1, Esr2a, or Esr2b expression construct. The cells were stimulated with different concentrations of E2 and luciferase activity was measured. (**D**) Effect of mutations in the ERE-like sequences on the E2-induced activation of *ara* transcription. Cultured cells were transfected with a wild-type luciferase construct or a construct carrying a mutation in the ERE-like sequence at position +1699 (mut+1699) or +2050 (mut+2050), together with an Esr1, Esr2a, or Esr2b expression construct. The cells were stimulated with or without E2, and luciferase activity was measured. (**E**) Ability of E2 to directly activate *arb* transcription. The assay described in C was performed with a luciferase construct containing a genomic fragment upstream of the first methionine codon of *arb*. (**F**) Effect of mutations in the ERE-like sequences on the E2-induced activation of *arb* transcription. The assay described in D was performed with luciferase constructs each carrying a mutation in the ERE-like sequence at position –1272 (mut-1272), –2180 (mut-2180), or –3327 (mut-3327). Values are expressed as a fold change relative to a control without E2 stimulation (C and E) or a control using the wild-type construct without E2 stimulation (D and F). Statistical differences were assessed by Dunnett's post hoc test (C and E) and unpaired *t* test with Bonferroni–Dunn correction (D and F). Error bars represent SEM.

815 **$P < 0.01$; ***$P < 0.001$.

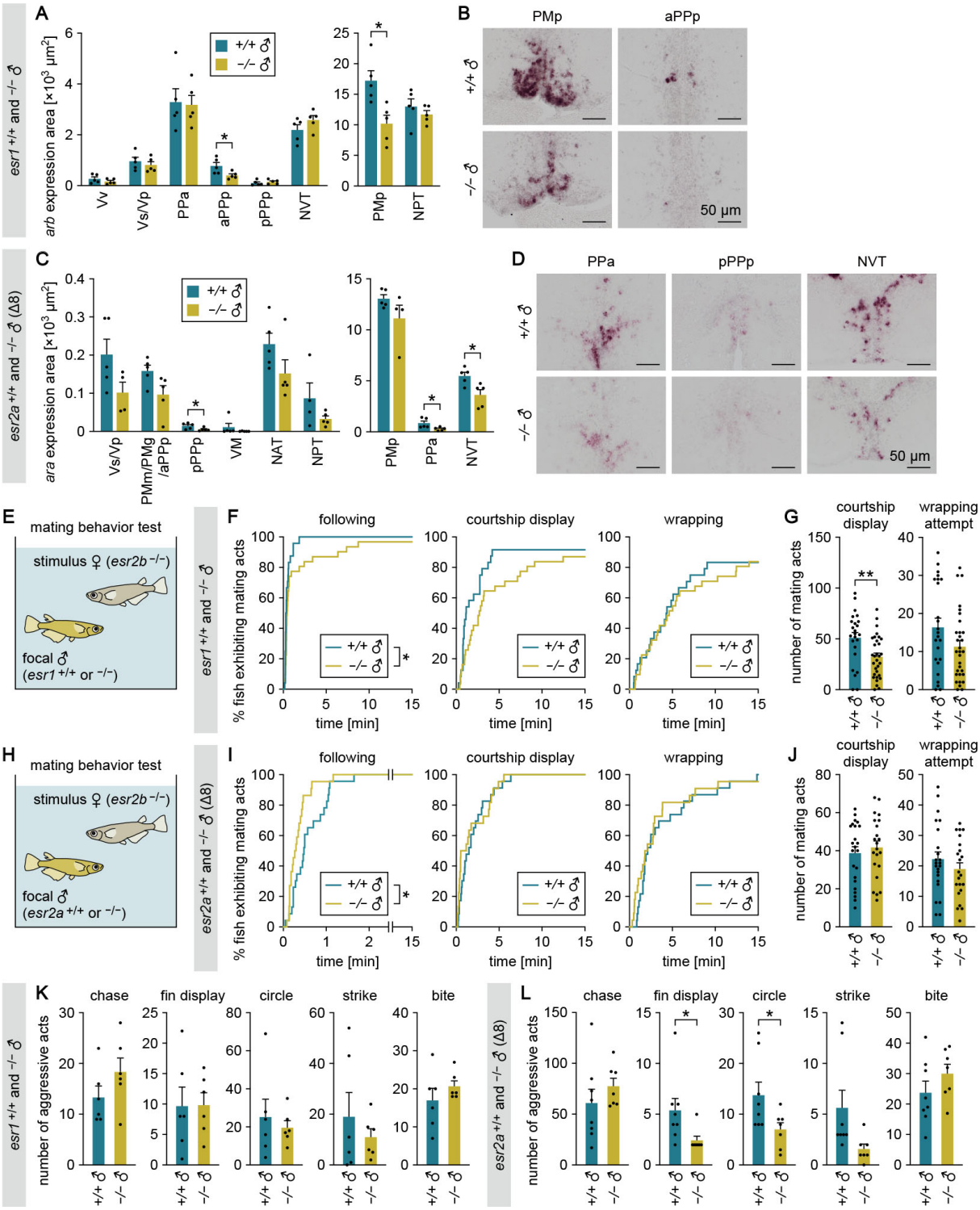

Fig. 5 Neuroestrogens stimulate *ara* and *arb* expression in behaviorally relevant brain regions primarily through Esr2a and Esr1, respectively.

(**A**) Total area of *arb* expression signal in each brain nucleus of $esr1^{+/+}$ and $esr1^{-/-}$ males (n = 5 per genotype). The data are displayed in two graphs for visual clarity. (**B**) Representative images of *arb* expression in the PMp and aPPp. (**C**) Total area of *ara* expression signal in each brain nucleus of $esr2a^{+/+}$ and $esr2a^{-/-}$ males (Δ8 line; n = 5 per genotype except for NPT of $esr2a^{+/+}$ males and Vs/Vp and PMp

824 of *esr2a*$^{-/-}$ males, where n = 4). The data are displayed in two graphs for visual clarity. (**D**)
825 Representative images of *ara* expression in the PPa, pPPp, and NVT. (**E**) Set-up for testing the mating
826 behavior of *esr1*$^{+/+}$ and *esr1*$^{-/-}$ males using an *esr2b*-deficient female as the stimulus. (**F**) Latency of
827 *esr1*$^{+/+}$ and *esr1*$^{-/-}$ males (n = 24 and 31, respectively) to initiate each mating act toward the stimulus
828 female. (**G**) Number of each mating act performed. (**H**) Set-up for testing the mating behavior of *esr2a*$^{+/+}$
829 and *esr2a*$^{-/-}$ males using an *esr2b*-deficient female as the stimulus. (**I**) Latency of *esr2a*$^{+/+}$ and *esr2a*$^{-/-}$
830 males (Δ8 line; n = 23 and 22, respectively) to initiate each mating act toward the stimulus female. (**J**)
831 Number of each mating act performed. (**K** and **L**) Total number of each aggressive act observed among
832 *esr1*$^{+/+}$ or *esr1*$^{-/-}$ males (n = 6 per genotype) (K) and among *esr2a*$^{+/+}$ or *esr2a*$^{-/-}$ males (Δ8 line; n = 8
833 and 7, respectively) (L) in the tank. Scale bars represent 50 μm. For abbreviations of brain nuclei, see
834 Table S1. Statistical differences were assessed by unpaired *t* test, with Welch's correction where
835 appropriate (A, C, G, J, K, and L) and Gehan-Breslow-Wilcoxon test (F and I). Error bars represent
836 SEM. *$P < 0.05$, **$P < 0.01$.

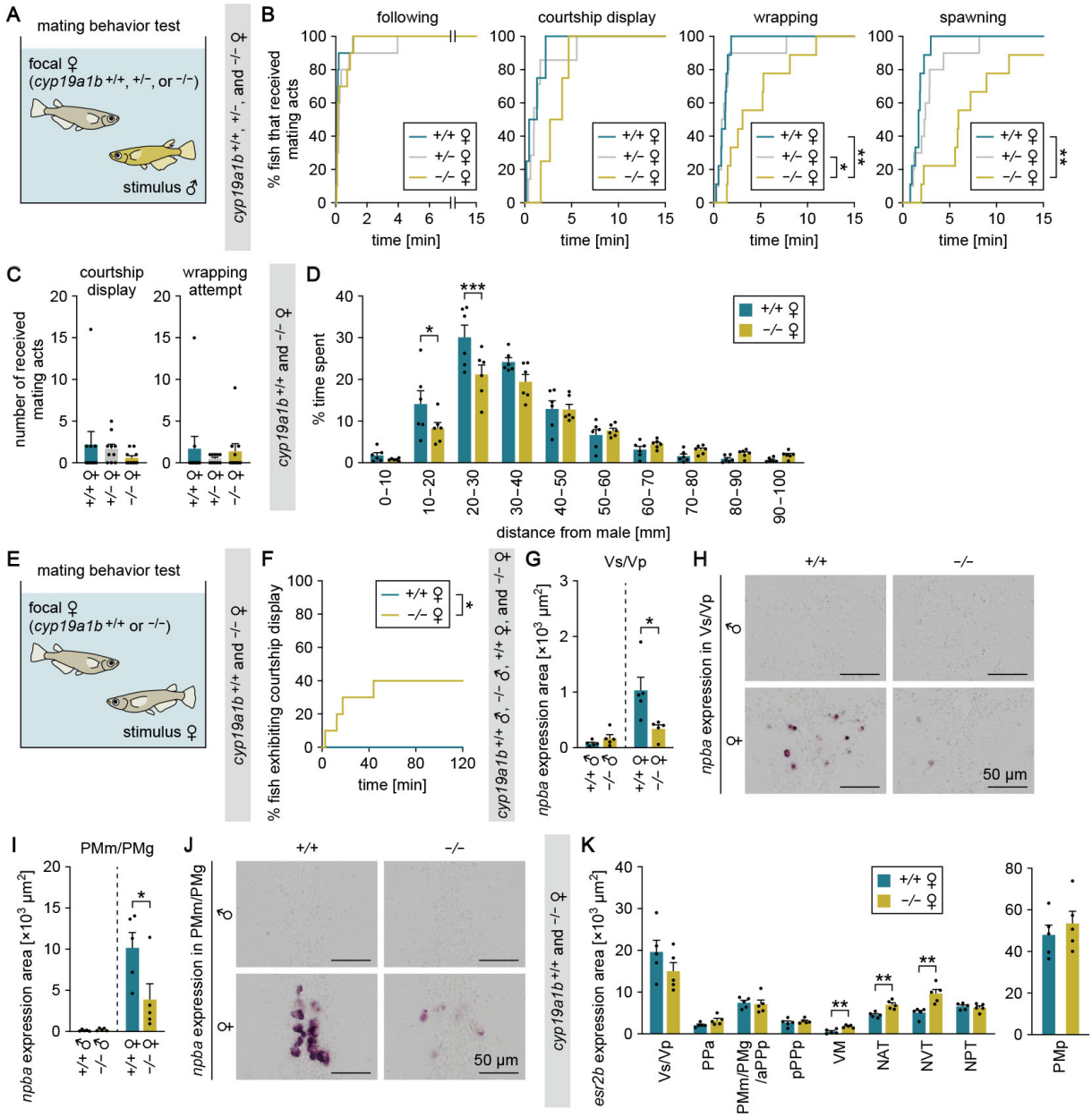

Fig. 6 *cyp19a1b*-deficient females are less receptive to males and instead court other females.

(**A**) Set-up for testing the mating behavior of *cyp19a1b*$^{+/+}$, *cyp19a1b*$^{+/-}$, and *cyp19a1b*$^{-/-}$ females. (**B**) Latency of *cyp19a1b*$^{+/+}$, *cyp19a1b*$^{+/-}$, and *cyp19a1b*$^{-/-}$ females (n = 10 per genotype) to receive each mating act from the stimulus male. (**C**) Number of each mating act received. (**D**) Percentage of time *cyp19a1b*$^{+/+}$ and *cyp19a1b*$^{-/-}$ females (n = 6 per genotype) spent at different distances from the stimulus male. (**E**) Set-up for testing the mating behavior of *cyp19a1b*$^{+/+}$ and *cyp19a1b*$^{-/-}$ females toward a stimulus female. (**F**) Latency of *cyp19a1b*$^{+/+}$ (n = 9) or *cyp19a1b*$^{-/-}$ (n = 10) females to initiate courtship displays toward the stimulus female. (**G** and **H**) Total area (G) and representative images (H) of *npba* expression signal in the Vs/Vp of *cyp19a1b*$^{+/+}$ and *cyp19a1b*$^{-/-}$ males and females (n = 5 per genotype and sex). (**I** and **J**) Total area (I) and representative images (J) of *npba* expression signal in the

850 PMm/PMg of *cyp19a1b*$^{+/+}$ and *cyp19a1b*$^{-/-}$ males and females (n = 5 per genotype and sex). (**K**) Total
851 area of *esr2b* expression signal in each brain nucleus of *cyp19a1b*$^{+/+}$ or *cyp19a1b*$^{-/-}$ females (n = 5 per
852 genotype). The data are displayed in two graphs for visual clarity. Scale bars represent 50 μm. For
853 abbreviations of brain nuclei, see Table S1. Statistical differences were assessed by Gehan-Breslow-
854 Wilcoxon test, with Bonferroni's correction where appropriate (B and F), Bonferroni's post hoc test (C),
855 unpaired *t* test with Bonferroni–Dunn correction (D), and unpaired *t* test, with Welch's correction where
856 appropriate (G, I, and K). Error bars represent SEM. *$P < 0.05$, **$P < 0.01$, ***$P < 0.001$.